Mechanism and Origins of Ligand-controlled Stereoselectivity of Ni-Catalyzed Suzuki-Miyaura Coupling with Benzylic Esters: A Computational Study

Shuo-Qing Zhang[†], **Buck L. H. Taylor**[‡,||], **Chong-Lei Ji**[†], **Yuan Gao**[†], **Michael R. Harris**[§], **Luke E. Hanna**[§], **Elizabeth R. Jarvo**[*,§], **K. N. Houk**[*,‡], and **Xin Hong**[*,†]

[†]Department of Chemistry, Zhejiang University, Hangzhou, 310027, China

[‡]Department of Chemistry and Biochemistry, University of California, Los Angeles, California 90095, United States

[§]Department of Chemistry, University of California, Irvine, California 92697, United States

[||]Department of Chemistry, Carleton College, Minnesota 55057, United States

Abstract

Nickel catalysts have shown unique ligand control of stereoselectivity in the Suzuki–Miyaura cross-coupling of boronates with benzylic pivalates and derivatives involving $C(sp^3)$–O cleavage. The SIMes ligand produces the stereochemically inverted C–C coupling product, while the PCy_3 ligand delivers the retained stereochemistry. We have explored the mechanism and origins of the ligand-controlled stereoselectivity with density functional theory (DFT) calculations. The oxidative addition determines the stereoselectivity with two competing transition states, an S_N2 back-side attack type transition state that inverts the benzylic stereogenic center, and a concerted oxidative addition through a cyclic transition state which provides stereoretention. The key difference between the two transition states is the substrate-nickel-ligand angle distortion; the ligand controls the selectivity by differentiating the ease of this angle distortion. For the PCy_3 ligand, the nickel-ligand interaction involves mainly σ-donation, which does not require a significant energy penalty for the angle distortion. The facile angle distortion with PCy_3 ligand allows the favorable cyclic oxidative addition transition state, leading to the stereoretention. For the SIMes ligand, the extra d-p back donation from nickel to the coordinating carbene increases the rigidity of nickel-ligand bond, and the corresponding angle distortion is more difficult. This makes the concerted cyclic oxidative addition unfavorable with SIMes ligand, and the back-side S_N2-type oxidative addition delivers the stereoinversion.
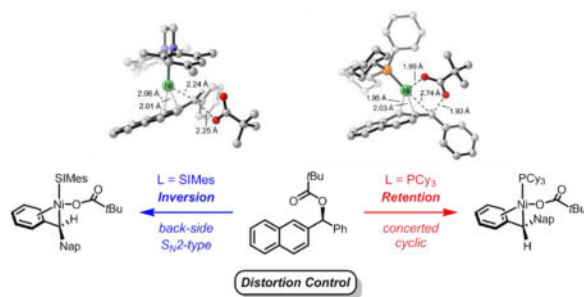
SYNOPSIS TOC

Introduction

Nickel-catalyzed cross-coupling reactions involving the C–O cleavage of esters provides a valuable tool to construct carboncarbon and carbon-heteroatom bonds in organic synthesis.[1] Based on early examples of Ni/PCy3-catalyzed Suzuki-Miyaura coupling with aryl esters,[2] the Ni-mediated $C(sp^2)$–O bond cleavage of ester[3] has been extended to various additional electrophiles, including carbamates,[4] sulfamates,[4c,4f,4g,5] phosphates,[6] and phenolates[7]. In addition, tremendous success has been achieved in the Nickel-catalyzed C–O activation and functionalization with ethers[8]. The judicious choice of nucleophiles in these reactions has enabled not only C–C bond formation, but also C–N, C–B, C–Si, C–H, C–P and C–Sn bond formations.[9] These transformations highlight the broad synthetic scope of Ni-mediated C–O cleavage of ester with distinctive reactivities and selectivities.

In 2011, Jarvo and co-workers reported the first stereospecific nickel-catalyzed alkyl-alkyl cross-coupling reaction via benzylic C–O cleavage.[10] This $C(sp^3)$–O cleavage provides the opportunity to control stereochemical outcome and led to a series of stereospecific cross-coupling reactions with benzylic and allylic esters and ethers.[11] A very selective inversion of the stereogenic center is found in most of the Ni-catalyzed cross-coupling reactions involving $C(sp^3)$–O cleavage, following the design of an S_N2-type bond activation. In addition to the selective inversion, Jarvo and co-workers reported a ligand-controlled stereoselectivity in nickel-catalyzed cross-coupling reactions with benzylic esters and derivatives (Scheme 1).[11d] The use of SIMes ligand (1,3-dimesityl-4,5-dihydroimidazol-2-ylidene) affords inversion at the benzylic carbon (Scheme 1a), while PCy3 ligand produces retention at the same position (Scheme 1b). Watson and co-workers concurrently reported Ni-catalyzed Suzuki-Miyaura coupling reactions that proceed with stereoinversion.[11e]

Although the mechanism and selectivities of Ni-mediated $C(sp^2)$–O cleavage of aryl esters and ethers have been addressed by several computational and experimental studies,[12] the model of bond activation and especially the origins of ligand-controlled stereoselectivity remain elusive for Ni-mediated $C(sp^3)$–O cleavage. Therefore, we have used density functional theory (DFT) calculations to explore the mechanism and the origins of the stereoselectivity of the titled reaction involving $C(sp^3)$–O activation. Understanding the ligand-controlled reversal of stereoselectivity will facilitate the development of new stereospecific and stereoconvergent reactions based on the Ni-mediated $C(sp^3)$–O activation.

Computational Methods

All DFT calculations were performed with the Gaussian 09 software package.[14] Geometry optimizations of all the minima and transition states were carried out at the B3LYP[15] level of theory with the LANL2DZ[16] basis set for nickel and the 6-31G(d) basis set for the other atoms (the keyword 5D was used in the calculations). Vibrational frequencies were computed at the same level to evaluate its zero-point vibrational energy (ZPVE) and thermal corrections at 298 K, and to check whether each optimized structure is an energy minimum or a transition state. The single-point energies and solvent effects in THF were computed at the M06[17] level of theory with the SDD[18] basis set for nickel and the 6-311+G(d,p) basis set for the other atoms, using the gas-phase optimized structures. Solvation energies were evaluated by a self-consistent reaction field (SCRF) using the CPCM model[19]. Several rotamers of ligands in the nickel complexes were tested as the initial geometry in the optimizations, and extensive conformational searches for the intermediates and transition states have been conducted. The lowest energy conformers and isomers are shown in this work. The 3D diagrams of molecules were generated using CYLView[20]. For the illustration of orbital interactions between ligands and nickel, natural bond orbital (NBO) population analysis was conducted with its supplement in Gaussian 09 (Version 3.1) at M06 level of theory with the def2-SVP[21] basis set and visualized with Multiwfn[22] and VMD[23].

Results and Discussion

Proposed catalytic cycle

Previous mechanistic studies[12,13] of aryl esters and ethers have shown that the Ni-catalyzed Suzuki-Miyaura coupling reaction proceeds via oxidative addition of the nickel catalyst to the substrate, followed by transmetallation with arylboronate and then reductive elimination to produce the coupling product and regenerate the active nickel catalyst. The transmetallation mainly involves bonding changes at the transition metal, instead of the adjacent stereogenic center, and reductive elimination typically occurs with stereochemical retention.[24] We propose that the reversal of stereoselectivity occurs at the oxidative addition step. As shown in Scheme 2, the two possible oxidative addition steps cleave the benzylic C–O bond of substrate **1**, leading to two LNi(Benzyl)(OPiv) intermediates with opposite configuration, **A** and **C**. Subsequent transmetallation with the arylboronate generates the corresponding LNi(Benzyl)(Ar) intermediates, **B** and **D**. From **B** or **D**, the reductive elimination occurs with retention and produces the enantiomeric C–C cross-coupling products, **2** and *ent*-**2**.

To study the proposed catalytic cycles and origins of stereoselectivity, particularly for comparison with previous computational studies on aryl pivalates,[4f, 12a] the reactions with benzyl pivalate **3** were chosen as our model reactions (Scheme 3, es values are defined as in Jarvo's previous study[11d]). With Ni/PCy$_3$ catalyst, stereoretention is observed, leading to product **4**; the Ni/SIMes catalyst delivers the stereoinverted product *ent*-**4**. Identical substrates are used in the computation with both ligands.

Free energy profile of the [Ni(PCy$_3$)]-catalyzed Suzuki-Miyaura coupling with benzylic pivalate

We first studied the Ni-catalyzed Suzuki-Miyaura coupling with benzylic ester **3** using PCy$_3$ ligand. The Gibbs free energy changes of the most favorable pathway that produces the stereoretentive product are shown in Figure 1, and the optimized structures of selected intermediates and transition states are illustrated in Figure 2. From the substrate-coordinated complex **5**, rotation of the benzylic substituents leads to the oxygen-coordinated intermediate **6**. This intermediate undergoes oxidative addition to cleave the benzylic C–O bond through a five-centered transition state **TS7**, generating the benzylnickel species **8** with stereoretention. Rotation of the newly formed Ni–C bond leads to a more stable intermediate **9**. The oxidative addition step is irreversible and requires a 17.7 kcal/mol barrier from intermediate **5** (stereoselectivity of the oxidative addition step is discussed later). The irreversible oxidative addition suggests that the transition state of this step determines the stereoselectivity of the C–O cleavage. We have also considered alternative C–O cleavages with Ni(I) catalysts, since Ni(0) and Ni(II) intermediates can potentially undergo comproportionation to generate Ni(I) species. The C–O cleavages with (PCy$_3$)Ni(OPiv) and (PCy$_3$)Ni(Benzyl) species both require much higher barrier as compared to the Ni(0)/Ni(II) process via **TS7** (Figure S1).

Subsequent to the oxidative addition, **9** undergoes a ligand exchange with the arylboronate [ArBnep(OH)]$^-$ to generate the intermediate **10**, and transmetallation via **TS11** gives the arylnickel species **12**.[25] Considering the existence of tBuO$^-$ and nBuO$^-$ anions in the reaction conditions, the transmetallations with [ArBnep(OnBu)]$^-$ and [ArBnep(OtBu)]$^-$ were also studied. For the [ArBnep(OnBu)]$^-$ anion, the transmetallation barrier is similar as compared to that with [ArBnep(OH)]$^-$ anion (Figure S2). This suggests that the [ArBnep(OnBu)]$^-$ can also participate in the transmetallation delivering the aryl group to nickel. In contrast, the transmetallation barriers with [ArBnep(OtBu)]$^-$ are much higher due to the steric repulsions between the tBu group and the bulky PCy$_3$ ligand (Figure S3). Therefore, the tBuO$^-$ anion probably acts as an off-cycle base, instead of directly participating in the transmetallation process.

From **12**, the boronate favorably dissociates from the complex, and the intermediate **13** undergoes reductive elimination via **TS14** to form the C(sp^3)–C(sp^2) bond and generate the product-coordinated complex **15**. The product can coordinate to nickel with either the phenyl group (**15**) or the naphthyl group (**16**), which have comparable stabilities. The optimized structures and relative stabilities of various product-nickel complexes are included in the Supporting Information (Figure S4). Both the product-nickel complexes can undergo a favorable ligand exchange with the benzylic ester substrate **3**, liberating the product **4** and initiating the next catalytic cycle.

In the catalytic cycle with PCy$_3$ ligand, the oxidative addition, transmetallation and reductive elimination all occur with stereoretention, and thus the stereoretentive C–C cross-coupling product **4** is produced. The on-cycle resting state is the substrate-coordinated complex **5** (we cannot rule out more stable off-cycle resting states), and the rate-limiting step is the oxidative addition via **TS7** with a 17.7 kcal/mol overall barrier. This 17.7 kcal/mol overall

barrier is consistent with the experimental conditions (room temperature, 20h)[11d]. In addition, although the overall transformation is quite exergonic by 47.8 kcal/mol, this does not create an inert nickel species which may limit the catalytic turnover. The free energy changes of two consecutive catalytic cycles showed that the regenerated substrate-nickel intermediate **5** is able to favorably undergo the next catalytic cycle, delivering the catalytic turnover (Figure S5).

Free energy profile of the [Ni(SIMes)]-catalyzed Suzuki-Miyaura coupling with benzylic ester

We next examined the Ni-catalyzed Suzuki-Miyaura coupling with benzylic ester **3** using SIMes ligand. The Gibbs free energy changes of the most favorable pathway that produces the product with stereoinversion are shown in Figure 3, and the optimized structures of selected intermediates and transition states are illustrated in Figure 4. From the substrate-coordinated complex **17**, a direct S_N2 attack from the nickel catalyst to the benzylic carbon occurs to produce a cationic benzylnickel species **19**. The ions recombine to form the intermediate **20** with an inverted benzylic stereogenic center. Similar to the PCy_3 ligand, the oxidative addition with SIMes ligand is also irreversible, suggesting that the stereoselectivity of this step is kinetically determined. We have also considered alternative C–O cleavage with Ni(I) catalysts. Similar to the PCy_3 ligand, the C–O cleavage barriers with (SIMes)Ni(OPiv) or (SIMes)Ni(Benzyl) species are both much higher than that of the Ni(0)/Ni(II) process via **TS18** (Figure S6).

From **20**, a ligand exchange with arylboronate [ArBnep(OH)]⁻ occurs to generate the intermediate **21**, and subsequent transmetallation occurs via **TS22** to give the arylnickel intermediate **23**. The transmetallation step with SIMes ligand (20.6 kcal/mol for **21** to **TS22**) requires a much higher barrier as compared to that with PCy_3 ligand (10.7 kcal/mol for **10** to **TS11**). This difference arises from the steric repulsion. In **TS22**, the benzyl group has steric repulsion with the SIMes ligand, while such steric interactions are alleviated with the conicalshaped PCy_3 ligand in **TS11**. The transmetallation with [ArBnep(O*n*Bu)]⁻ has a comparable barrier as compared to that with [ArBnep(OH)]⁻ via **TS22** (Figure S7), while the transmetallation with [ArBnep(O*t*Bu)]⁻ requires a much higher barrier (Figure S8). These results with SIMes ligand are similar to the results with PCy_3 ligand in the above discussions.

For the $C(sp^3)$–$C(sp^2)$ reductive elimination step, the kinetics shows low sensitivity to the ligand, both PCy_3 and SIMes ligands have about a barrier of 13 kcal/mol. The various conformers of the product-nickel complex have similar stabilities (Figure S9), and both **26** and **27** can undergo a favorable product liberation to produce the stereoinverted $C(sp^3)$–$C(sp^2)$ coupling product *ent*-**4**. For the catalytic cycle with SIMes ligand, the oncycle resting state is intermediate **20**, and the rate-determining step is transmetallation via **TS22** with a 21.7 kcal/mol overall barrier. This reaction barrier is consistent with the mild reaction conditions (room temperature, 20h)[11d]. In addition, the exergonicity of the overall transformation (47.8 kcal/mol) does not affect the catalytic turnover, since no catalyst-poisoning species are involved. The free energy changes of two consecutive catalytic cycles

showed that the regenerated substrate-nickel intermediate **17** is able to favorably undergo the subsequent catalytic cycle, and the catalytic turnover is achieved (Figure S10).

Origins of the opposite stereoselectivities of the reactions with different ligands

Based on the mechanistic understandings of PCy_3 and SIMes ligands, we studied the origins of the ligand-controlled stereoselectivity by comparing the invertive and retentive oxidative addition pathways. The results are shown in Figure 5. For PCy_3 ligand, the substrate-coordinated complex, **5**, can undergo an oxidative addition via transition state **TS28** with stereoinversion (blue pathway). **TS28** is essentially an S_N2 back-side attack transition state; the nickel catalyst attacks the benzylic carbon from the back side of the leaving pivalate group, inverting the benzylic stereogenic center. Alternatively, **5** can isomerize to the six-membered ring intermediate **6** and undergoes the oxidative addition via transition state **TS7** with stereochemical retention (red pathway). **TS7** is a concerted cyclic oxidative addition transition state, wherein the nickel catalyst interacts with the benzylic carbon and cleaves the C–O bond on the same side. This transition state allows retention of the benzylic stereogenic center and irreversibly produces the benzylnickel intermediate **9**. Comparing the two pathways with PCy_3 ligand, the retention pathway via **TS7** is 1.1 kcal/mol more favorable than the inversion pathway via **TS28**. This agrees well with the experimental preference of stereoretention with PCy_3 ligand (Scheme 3a). For SIMes ligand, the stereoselectivity is reversed. The inversion pathway via **TS18** is 1.6 kcal/mol more favorable as compared to the retention pathway via **TS32**, which also agrees with the experimental results (Scheme 3b). To further validate this mechanistic model, we also studied the stereoselectivity with benzyl carbamates. Experimentally, these carbamates showed better yields as well as higher stereoselectivity.[11d] The computational results based on the inversion/retention oxidative addition model also nicely reproduced the above trends with somewhat higher stereoselectivity (Figure S11), which provide additional support for the proposed mechanistic rationale.

To elucidate the origins of the ligand-controlled stereoselectivity, we analyzed these two free energy surfaces based on Curtin-Hammett principle. The Curtin-Hammett principle states that the stereoselectivity is only controlled by the competition between the determining transition states (**TS28** vs. **TS7**; **TS18** vs. **TS32**). Using the PCy_3 ligand as an example, the stereoselectivity is determined as eqn 1 (Scheme 4). In addition, the free energies of the determining transition states ($\Delta G^{\ddagger}$(**TS28**) and $\Delta G^{\ddagger}$(**TS7**)) can further be expressed as the sum of the free energies of the preceding intermediates (ΔG(**5**) and ΔG(**6**)) and the intrinsic reaction barriers ($\Delta G^{\ddagger}$(**5**→**TS28**) and $\Delta G^{\ddagger}$(**6**→**TS7**)), which are shown as eqn 2 and eqn 3 in Scheme 4. Combining these three equations, the stereoselectivity is contributed by the intrinsic reaction barriers of inversion and retention, as well as the isomerization energy between **5** and **6** (eqn 4, Scheme 4).

Following the analysis based on the Curtin-Hammett principle, we decomposed the stereoselectivity ($\Delta\Delta G^{\ddagger}$) to the contributions of intrinsic oxidative addition barriers and isomerization energy between the preceding intermediates (Table 1). The intrinsic barriers of inversion and retention barely change between the PCy_3 and SIMes ligands, while the isomerization energy (ΔG_{iso}) increases by 2.2 kcal/mol from PCy_3 to SIMes ligand. This 2.2

kcal/mol difference of isomerization energy affects the energies of the invertive and retentive oxidative addition transition states, altering the stability of these transition states and eventually switching the stereoselectivity. Therefore, the intrinsic barrier favors the retention pathway for both ligands, and the major contribution to the switch of selectivity is the change of the isomerization energy between the two oxidative addition preceding intermediates.

To further understand the origins of the ligand effects, we analyzed the ligand effects on the isomerization energy by comparing the energies of the distorted fragments in the two oxidative addition preceding intermediates (Figure 6). We first calculated the electronic energies of the intermediates. With SIMes ligand, the isomerization from pre-inversion intermediates to pre-retention intermediates is less favorable as compared to PCy_3 ligand (2.2 kcal/mol in terms of free energy and 2.4 kcal/mol in terms of electronic energy). To understand which part of the complex is responsible for the ligand effects, we replaced the acyl moiety (highlighted with dashed green oval) in the four intermediates with a hydrogen atom[26], and calculated the energies of the four distorted fragments. The electronic energy difference between the two fragments with PCy_3 ligand, **5-1** and **6-1**, is 9.4 kcal/mol, and that with SIMes ligand is 11.6 kcal/mol. The change is 2.2 kcal/mol, similar to the 2.4 kcal/mol energy difference with the whole complex, suggesting that the acyl moiety is not responsible for the ligand control. In addition, when the benzyl moiety is replaced by hydrogen atom[27], surprisingly, the ligand effects still exist. The energy change between **5-2** and **6-2** is 4.2 kcal/mol, and that between **17-2** and **31-2** is 6.1 kcal/mol. Thus the LNi(napthyl) moiety plays a critical role in differentiating the isomerization energy. The major geometric change in the LNi(napthyl) moiety in the bending of the highlighted C-Ni-Ligand angle. From the pre-inversion intermediate (**5** or **17**) to the pre-retention intermediate (**6** or **31**), the complex bends the C-Ni-Ligand angle to accommodate the formation of the additional Ni–O bond. This bending is easier with PCy_3 ligand (4.2 kcal/mol) as compared to SIMes ligand (6.1 kcal/mol). Therefore, the ligand controls the stereoselectivity by controlling the ease of distortion of the highlighted C-Ni-Ligand angle.

We hypothesized that the rigidity of the Ni–ligand bond determines the ease of the angle distortion, and analyzed the related interactions with d orbital of nickel in the [LNi(naphthalene)] complexes (results shown in Figure 7). The PCy_3 ligand interacts with nickel mainly through σ-donation, and this Ni-PCy_3 interaction does not change significantly during the bending of the highlighted C-Ni-ligand angle, resulting in a small energy penalty for the angle distortion. For SIMes ligand, the ligand-metal interaction also includes an additional d-p back donation,[28] which is not present in the Ni–PCy_3 bond. This makes the Ni–NHC bond a partial double bond. In addition, the d orbital of nickel also interacts with π^* orbital of the naphthalene in both complexes. Thus, the d orbital of nickel in the [(NHC)Ni(substrate)] complex is orientated to maximize the overlap with the p orbital of the NHC ligand as well as the π^* orbital of the naphthalene moiety. Bending of the C-Ni-NHC angle therefore weakens the d-p_{ligand} back donation, resulting in a larger energy penalty for the angle distortion as compared to PCy_3 ligand.

To verify our hypothesis, we studied the bending of the C-Ni-ligand angle with a few [LNi(naphthalene)] complexes. Four ligands were chosen: PCy_3, SIMes, PMe_3 and 1,3-

dimethyl-imidazolidene (SIMe). The [LNi(naphthalene)] complexes were optimized, giving an initial C-Ni-ligand angle. This angle was then decreased (as it must to accommodate coordination of the pivalate) and the change in electronic energy was calculated (Figure 8). Indeed, the bending of the substrate-Ni-SIMes angle is more difficult than that of the substrate-Ni-PCy$_3$ angle, which confirms the above hypothesis of the ligand-dependent ease of angle distortion. In addition, the comparison between the small PMe$_3$ and SIMe ligands shows that the PMe$_3$ ligand is also easier to bend as compared to SIMe ligand, similar to the difference between PCy$_3$ and SIMes ligands. This is consistent with the rationale relying on the intrinsic orbital interaction.

Because we hypothesized that the d-$\pi^*$$_{naphthalene}$ interactions between nickel and naphthalene orient the d orbital of nickel to make bending more difficult with the NHC ligand than with the phosphine ligand, these effects would be eliminated if the naphthalene coordination is replaced with a σ-donating ligand. To verify this hypothesis, we also calculated the energy changes of the angle distortion using [LNi(NH$_3$)] complex (Figure 9). The NH$_3$ ligand mainly interacts with nickel through σ-donation and has little effect on the orientation of nickel d orbitals. As expected, all four ligands have almost identical energy penalties for angle distortion. This suggests that the PCy$_3$ and SIMes ligands should have similar preference for the S$_N$2-type transition state if a substrate interacts with nickel through an NH$_2$-coordination. Indeed, the C–O cleavage of (S)-2-amino-1-phenylethyl pivalate **35** showed very similar selectivity for the PCy$_3$ and SIMes ligands (Figure 10); both ligands strongly favor the S$_N$2-type C–O cleavage transition state. These results provide further support that the bending of the substrate-nickelligand angle controls the stereoselectivity.

In addition to the electronic effects, steric effects can also play a role in affecting the stereoselectivity. To elucidate the steric effects of the pivalate substrate, we studied the stereoselectivity with additional methyl substituent on each position of the naphthyl group of **3** (Table 2A). For most positions (2-Me to 7-Me), the additional methyl substituent has limited effects on the stereoselectivity, and the trends are very similar to the unsubstituted cases (PCy$_3$ ligand favors retention and SIMes ligand favors inversion). However, for position 1, the steric repulsions between the introduced methyl substituent and the adjacent phenyl group disfavor the inversion transition state, and both ligands now favor the retention pathway. The steric repulsions with the methyl substituent in position 1 are illustrated in the Supporting Information (Figure S12). Thus, the steric effects of this particular position can have significant effects on the stereoselectivity. For the steric effects of the ligand, the PCy$_3$ and SIMes ligands were compared to two additional ligands with more steric bulk: PtBu$_3$ and SIPr. These larger ligands strongly favor the inversion pathway, because of steric repulsions between the pivalate group and the ligand in the retentive oxidative addition transition states (Table 2B). The illustrations of the steric repulsions in the transition states with PtBu$_3$ and SIPr ligands are included in the Supporting Information (Figure S13).

Conclusions

The mechanism and origins of the ligand-controlled stereoselectivity of Ni-catalyzed Suzuki-Miyaura coupling of benzylic pivalates have been elucidated with DFT calculations.

The reaction proceeds through the oxidative addition of the nickel catalyst and benzylic $C(sp^3)$–O bond cleavage. The generated [LNi(II)(benzyl)(OPiv)] intermediate undergoes transmetallation with arylboronate and subsequent C–C reductive elimination to produce the $C(sp^3)$–$C(sp^2)$ cross-coupling product. The transmetallation and reductive elimination both occur with stereochemical retention, and the stereoselectivity of the oxidative addition step determines the overall stereochemical outcome of the cross-coupling reaction. The stereoselectivity of oxidative addition is determined by two competing transition states: an S_N2-type transition state in which the nickel attacks the benzylic carbon from the back side of the pivalate leaving group, inverting the benzylic stereogenic center; and a concerted oxidative addition through a cyclic transition state in which the nickel interacts with the pivalate carbonyl oxygen while cleaving the benzylic $C(sp^3)$–O bond, generating a benzylnickel complex with stereochemical retention.

The relative energies of the intermediates preceding the oxidative addition transition states, as well as the subsequent transition states, controls the ligand-dependent stereoselectivity. The key difference between the two intermediates and two transition states is the bending of substrate-nickel-ligand angle. The intermediate for the stereochemical inversion $C(sp^3)$–O cleavage has nickel on the opposite side of the leaving pivalate group and does not bend the substrate-nickel-ligand angle significantly, while the intermediate for the stereochemical retention $C(sp^3)$–O cleavage bends the substrate-nickel-ligand angle to accommodate an additional nickel-oxygen(pivalate) interaction. This bending is facile with phosphine ligand since the ligand interacts with nickel mainly through σ-donation; with NHC ligand, the same angle distortion is more difficult because the nickel-ligand bond is partially a double bond due to the d-p interaction between nickel and the NHC ligand. The ligand-dependent substrate-nickel-ligand angle distortion results in the different energies of the competing oxidative addition transition states, ultimately leading to the reversal of stereoselectivities. In addition to the electronic effects, the steric effects can also affect the stereoselectivity. Ligands with more steric bulk disfavor the retention pathway due to the steric repulsions between the pivalate group of the substrate and the ligand. These mechanistic insights apply to the related stereospecific cross-coupling reactions and other transformations involving nickel-mediated $C(sp^3)$–O cleavage.

Supplementary Material

Refer to Web version on PubMed Central for supplementary material.

Acknowledgments

References

1. For reviews, see: Yu D-G, Li B-J, Shi Z-J. Acc. Chem. Res. 2010; 43:1486. [PubMed: 20849101] Rosen BM, Quasdorf KW, Wilson DA, Zhang N, Resmerita A-M, Garg NK, Percec V. Chem. Rev.

2011; 111:1346. [PubMed: 21133429] Han F-S. Chem. Soc. Rev. 2013; 42:5270. [PubMed: 23460083] Yamaguchi J, Muto K, Itami K. Eur. J. Org. Chem. 2013; 2013:19.Mesganaw T, Garg NK. Org. Process Res. Dev. 2013; 17:29.Tasker SZ, Standley EA, Jamison TF. Nature. 2014; 509:299. [PubMed: 24828188] Tobisu M, Chatani N. Top. Curr. Chem. 2016; 374:41.Zeng H, Qiu Z, Domínguez-Huerta A, Hearne Z, Chen Z, Li C-J. ACS Catal. 2017; 7:510.

2. (a) Quasdorf KW, Tian X, Garg NK. J. Am. Chem. Soc. 2008; 130:14422. [PubMed: 18839946] (b) Guan B-T, Wang Y, Li B-J, Yu D-G, Shi Z-J. J. Am. Chem. Soc. 2008; 130:14468. [PubMed: 18847272]

3. (a) Shimasaki T, Tobisu M, Chatani N. Angew. Chem. Int. Ed. 2010; 49:2929.(b) Ehle AR, Zhou Q, Watson MP. Org. Lett. 2012; 14:1202. [PubMed: 22335199] (c) Muto K, Yamaguchi J, Itami K. J. Am. Chem. Soc. 2012; 134:169. [PubMed: 22148419] (d) Wang J, Ferguson DM, Kalyani D. Tetrahedron. 2013; 69:5780.(e) Takise R, Muto K, Yamaguchi J, Itami K. Angew. Chem. Int. Ed. 2014; 53:6791.(f) Zarate C, Martin R. J. Am. Chem. Soc. 2014; 136:2236. [PubMed: 24476124] (g) Koch E, Takise R, Studer A, Yamaguchi J, Itami K. Chem. Commun. 2015; 51:855.(h) Correa A, Leon T, Martin R. J. Am. Chem. Soc. 2014; 136:1062. [PubMed: 24377699] (i) Kinuta H, Hasegawa J, Tobisu M, Chatani N. Chem. Lett. 2015; 44:366.(j) Yang J, Chen T, Han L-B. J. Am. Chem. Soc. 2015; 137:1782. [PubMed: 25629169] (k) Cornella J, Jackson EP, Martin R. Angew. Chem. Int. Ed. 2015; 54:4075.(l) Muto K, Hatakeyama T, Yamaguchi J, Itami K. Chem. Sci. 2015; 6:6792.(m) Yang J, Xiao J, Chen T, Han L-BJ. J. Org. Chem. 2016; 81:3911. [PubMed: 27055171] (n) Guo L, Hsiao C-C, Yue H, Liu X, Rueping M. ACS Catal. 2016; 6:4438.(o) Gu Y, Martin R. Angew. Chem. Int. Ed. 2017; 56:3187.(p) Yue H, Guo L, Liao H-H, Cai Y, Zhu C, Rueping M. Angew. Chem. Int. Ed. 2017; 56:4282.(q) Yue H, Guo L, Liu X, Rueping M. Org. Lett. 2017; 19:1788. [PubMed: 28287744]

4. (a) Sengupta S, Leite M, Raslan DS, Quesnelle C, Snieckus V. J. Org. Chem. 1992; 57:4066.(b) Dallaire C, Kolber I, Gingras M. Org. Synth. 2002; 78:42.(c) Quasdorf KW, Riener M, Petrova KV, Garg NK. J. Am. Chem. Soc. 2009; 131:17748. [PubMed: 19928764] (d) Antoft-Finch A, Blackburn T, Snieckus V. J. Am. Chem. Soc. 2009; 131:17750. [PubMed: 19928763] (e) Xi L, Li B-J, Wu Z-H, Lu X-Y, Guan B-T, Wang B-Q, Zhao K-Q, Shi Z-J. Org. Lett. 2010; 12:884. [PubMed: 20099867] (f) Quasdorf KW, Antoft-Finch A, Liu P, Silberstein AL, Komaromi A, Blackburn T, Ramgren SD, Houk KN, Snieckus V, Garg NK. J. Am. Chem. Soc. 2011; 133:6352. [PubMed: 21456551] (g) Mesganaw T, Silberstein AL, Ramgren SD, Nathel NFF, Hong X, Liu P, Garg NK. Chem. Sci. 2011; 2:1766.(h) Mesganaw T, Nathel NFF, Garg NK. Org. Lett. 2012; 14:2918. [PubMed: 22612586] (i) Hie L, Ramgren SD, Mesganaw T, Garg NK. Org. Lett. 2012; 14:4182. [PubMed: 22849697] (j) Ramgren SD, Hie L, Ye Y-X, Garg NK. Org. Lett. 2013; 15:3950. [PubMed: 23879392] (k) Ohtsuki A, Yanagisawa K, Furukawa T, Tobisu M, Chatani N. J. Org. Chem. 2016; 81:9409. [PubMed: 27603684] (l) Takise R, Itami K, Yamaguchi J. Org. Lett. 2016; 18:4428. [PubMed: 27518123] (m) Wang Y, Wu SB, Shi WJ, Shi ZJ. Org. Lett. 2016; 18:2548. [PubMed: 27205866] (n) Shi W-J, Zhao H-W, Wang Y, Cao Z-C, Zhang L-S, Yu D-G, Shi Z-J. Adv. Synth. Catal. 2016; 358:2410.

5. (a) Macklin TK, Snieckus V. Org. Lett. 2005; 7:2519. [PubMed: 15957880] (b) Wehn PM, Du Bois J. Org. Lett. 2005; 7:4685. [PubMed: 16209510] (c) Ramgren SD, Silberstein AL, Yang Y, Garg NK. Angew. Chem. Int. Ed. 2011; 50:2171.(d) Ackermann L, Sandmann R, Song W. Org. Lett. 2011; 13:1784. [PubMed: 21351758] (e) Chen G-J, Han F-S. Eur. J. Org. Chem. 2012; 2012:3575. (f) Leowanawat P, Zhang N, Safi M, Hoffman DJ, Fryberger MC, George A, Percec V. J. Org. Chem. 2012; 77:2885. [PubMed: 22369478] (g) Ke H, Chen X, Zou G. J. Org. Chem. 2014; 79:7132. [PubMed: 25025343] (h) Park NH, Teverovskiy G, Buchwald SL. Org. Lett. 2014; 16:220. [PubMed: 24283652] (i) Mohadjer Beromi M, Nova A, Balcells D, Brasacchio AM, Brudvig GW, Guard LM, Hazari N, Vinyard DJ. J. Am. Chem. Soc. 2017; 139:922. [PubMed: 28009513]

6. (a) Chen H, Huang Z-B, Hu X-M, Tang G, Xu P-X, Zhao Y-F, Cheng C-H. J. Org. Chem. 2011; 76:2338. [PubMed: 21388215] (b) Huang J-H, Yang LM. Org. Lett. 2011; 13:3750. [PubMed: 21688805] (c) Xing T, Zhang Z, Da Y–X, Quan Z–J, Wang X–C. Tetrahedron Lett. 2015; 56:6495.

7. (a) Yu D-G, Li B-J, Zheng S-F, Guan B-T, Wang B-Q, Shi Z-J. Angew. Chem. Int. Ed. 2010; 49:4566.(b) Yu D-G, Shi Z-J. Angew. Chem. Int. Ed. 2011; 50:7097.

8. Dankwardt JW. Angew. Chem. Int. Ed. 2004; 43:2428.Tobisu M, Shimasaki T, Chatani N. Angew. Chem. Int. Ed. 2008; 47:4866.Shimasaki T, Konno Y, Tobisu M, Chatani N. Org. Lett. 2009; 11:4890. [PubMed: 19810683] Tobisu M, Shimasaki T, Chatani N. Chem. Lett. 2009;

38:710.Álvarez-Bercedo P, Martin R. J. Am. Chem. Soc. 2010; 132:17352. [PubMed: 20843037] Xie L-G, Wang Z-X. Chem. Eur. J. 2011; 17:4972. [PubMed: 21365710] Tobisu M, Chatani N. ChemCatChem. 2011; 3:1410.Sergeev AG, Hartwig JF. Science. 2011; 332:439. [PubMed: 21512027] Iglesias MJ, Prieto A, Nicasio MC. Org. Lett. 2012; 14:4318. [PubMed: 22894704] Tobisu M, Yasutome A, Yamakawa K, Shimasaki T, Chatani N. Tetrahedron. 2012; 68:5157.Cornella J, Gómez-Bengoa E, Martin R. J. Am. Chem. Soc. 2013; 135:1997. [PubMed: 23316793] Tobisu M, Yasutome A, Kinuta H, Nakamura K, Chatani N. Org. Lett. 2014; 16:5572. [PubMed: 25325885] Leiendecker M, Hsiao C-C, Guo L, Alandini N, Rueping M. Angew. Chem. Int. Ed. 2014; 53:12912.Tobisu M, Takahira T, Ohtsuki A, Chatani N. Org. Lett. 2015; 17:680. [PubMed: 25584633] Tobisu M, Chatani N. Acc. Chem. Res. 2015; 48:1717. [PubMed: 26036674] Zarate C, Manzano R, Martin R. J. Am. Chem. Soc. 2015; 137:6754. [PubMed: 25978094] Tobisu M, Zhao J, Kinuta H, Furukawa T, Igarashi T, Chatani N. Adv. Synth. Catal. 2016; 358:2417.For some related formal C–O bond activation of via Ni-catalysis, see: Graham TJA, Doyle AG. Org. Lett. 2012; 14:1616. [PubMed: 22385385] Sylvester KT, Wu K, Doyle AG. J. Am. Chem. Soc. 2012; 134:16967. [PubMed: 23030789]

9. For selected examples on C–C bond formation, see: ref 3b–3e, 3g, 3h, 3k, 3l, 3n, 4a–f, 7a, 7b, 8a–e, and 8h. For selected examples on C–N bond formation, see: ref 3a, 3p, 3q, 4g, 4i, 5c, 5d, 5h, 6b, and 8d. For selected examples on C–B bond formation, see: ref 3i, 8p and 8q. For an example on C–Si bond formation, see: ref 3f. For selected examples on C–H bond formation, see: ref 4h, 8e, 8g, 8h, and 8k. For selected examples on C–P bond formation, see: ref 3j and 3m. For a recent example on C–Sn bond formation, see: 3o.

10. Taylor BLH, Swift EC, Waetzig JD, Jarvo ER. J. Am. Chem. Soc. 2011; 133:389. [PubMed: 21155567]

11. Taylor BLH, Jarvo ER. Synlett. 2011; 19:2761.Greene MA, Yonova IM, Williams FJ, Jarvo ER. Org. Lett. 2012; 14:4293. [PubMed: 22568515] Taylor BLH, Harris MR, Jarvo ER. Angew. Chem. Int. Ed. 2012; 51:7790.Harris MR, Hanna LE, Greene MA, Moore CE, Jarvo ER. J. Am. Chem. Soc. 2013; 135:3303. [PubMed: 23414579] Zhou Q, Srinivas HD, Dasgupta S, Watson MP. J. Am. Chem. Soc. 2013; 135:3307. [PubMed: 23425080] Wisniewska HM, Swift EC, Jarvo ER. J. Am. Chem. Soc. 2013; 135:9083. [PubMed: 23751004] Yonova IM, Johnson AG, Osborne CA, Moore CE, Morrissette NS, Jarvo ER. Angew. Chem. Int. Ed. 2014; 53:2422.Harris MR, Konev MO, Jarvo ER. J. Am. Chem. Soc. 2014; 136:7825. [PubMed: 24852707] Tollefson EJ, Dawson DD, Osborne CA, Jarvo ER. J. Am. Chem. Soc. 2014; 136:14951. [PubMed: 25308512] Srinivas HD, Zhou Q, Watson MP. Org. Lett. 2014; 16:3596. [PubMed: 24927013] Johnson AG, Tranquilli MM, Harris MR, Jarvo ER. Tetrahedron Lett. 2015; 56:3486. [PubMed: 26085695] Tollefson EJ, Hanna LE, Jarvo ER. Acc. Chem. Res. 2015; 48:2344. [PubMed: 26197033] Tollefson EJ, Erickson LW, Jarvo ER. J. Am. Chem. Soc. 2015; 137:9760. [PubMed: 26230365] Dawson DD, Jarvo ER. Org. Proc. Res. Dev. 2015; 19:1356.Zhou Q, Srinivas HD, Zhang S, Watson MP. J. Am. Chem. Soc. 2016; 138:11989. [PubMed: 27589327] Zhou Q, Cobb KM, Tan T, Watson MP. J. Am. Chem. Soc. 2016; 138:12057. [PubMed: 27610831] Erickson LW, Lucas EL, Tollefson EJ, Jarvo ER. J. Am. Chem. Soc. 2016; 138:14006.Guo Y-A, Liang T, Kim SK, Xiao H, Krische MJ. J. Am. Chem. Soc. 2017; 139:6847. [PubMed: 28489371] For a recent deoxygenation of ethers involving Ni-catalyzed benzylic C–O cleavage, see: Cao Z-C, Shi Z-J. J. Am. Chem. Soc. 2017; 139:6546. [PubMed: 28445066]

12. For mechanistic studies on Ni-mediated C(sp^2)–O cleavage, see: Li Z, Zhang S-L, Fu Y, Guo Q-X, Liu L. J. Am. Chem. Soc. 2009; 131:8815. [PubMed: 19505075] Hong X, Liang Y, Houk KN. J. Am. Chem. Soc. 2014; 136:2017. [PubMed: 24428154] Lu Q, Yu H, Fu Y. J. Am. Chem. Soc. 2014; 136:8252. [PubMed: 24823646] Xu H, Muto K, Yamaguchi J, Zhao C, Itami K, Musaev DG. J. Am. Chem. Soc. 2014; 136:14834. [PubMed: 25259782] Muto K, Yamaguchi J, Musaev DG, Itami K. Nature Commun. 2015; 6:7508. [PubMed: 26118733] Ogawa H, Minami H, Ozaki T, Komagawa S, Wang C, Uchiyama M. Chem. Eur. J. 2015; 21:13904. [PubMed: 26294322] Durr AB, Yin G, Kalvet I, Napoly F, Schoenebeck F. Chem. Sci. 2016; 7:1076.Liu X, Hsiao C-C, Kalvet I, Leiendecker M, Guo L, Schoenebeck F, Rueping M. Angew. Chem. Int. Ed. 2016; 55:6093.and ref 4f, 4g. For other related mechanistic studies, see: Yoshikai N, Matsuda H, Nakamura E. J. Am. Chem. Soc. 2008; 130:15258. [PubMed: 18950159] Yoshikai N, Matsuda H, Nakamura E. J. Am. Chem. Soc. 2009; 131:9590. [PubMed: 19522507] Xue L-Q, Lin Z-Y. Chem. Soc. Rev. 2010; 39:1692. [PubMed: 20419215] Li Z, Jiang Y-Y, Fu Y. Chem. Eur. J. 2012; 18:4345. [PubMed: 22374716] Yu H-Z, Fu Y. Chem. Eur. J. 2012; 18:16765. [PubMed: 23112051]

Li Z, Liu L. Chin. J. Catal. 2015; 36:3.Bajo S, Laidlaw G, Kennedy AR, Sproules S, Nelson DJ. Organometallics. 2017; 36:1662.

13. For related mechanistic studies involving Ni(0)/Ni(II) catalytic cycles with Ni/NHC catalysts, see: Doster ME, Johnson SA. Angew. Chem. Int. Ed. 2009; 48:2185.Xu L, Chung LW, Wu Y-D. ACS Catal. 2016; 6:483.Ritleng V, Henrion M, Chetcuti MJ. ACS Catal. 2016; 6:890.Menezes da Silva VH, Braga AAC, Cundari TR. Organometallics. 2016; 35:3170.and ref 4g.

14. Frisch, MJ., Trucks, GW., Schlegel, HB., Scuseria, GE., Robb, MA., Cheeseman, JR., Scalmani, G., Barone, V., Mennucci, B., Petersson, GA., Nakatsuji, H., Caricato, M., Li, X., Hratchian, HP., Izmaylov, AF., Bloino, J., Zheng, G., Sonnenberg, JL., Hada, M., Ehara, M., Toyota, K., Fukuda, R., Hasegawa, J., Ishida, M., Nakajima, T., Honda, Y., Kitao, O., Nakai, H., Vreven, T., Montgomery, JA., Jr, Peralta, JE., Ogliaro, F., Bearpark, M., Heyd, JJ., Brothers, E., Kudin, KN., Staroverov, VN., Kobayashi, R., Normand, J., Raghavachari, K., Rendell, A., Burant, JC., Iyengar, SS., Tomasi, J., Cossi, M., Rega, N., Millam, JM., Klene, M., Knox, JE., Cross, JB., Bakken, V., Adamo, C., Jaramillo, J., Gomperts, R., Stratmann, RE., Yazyev, O., Austin, AJ., Cammi, R., Pomelli, C., Ochterski, JW., Martin, RL., Morokuma, K., Zakrzewski, VG., Voth, GA., Salvador, P., Dannenberg, JJ., Dapprich, S., Daniels, AD., Farkas, O., Foresman, JB., Ortiz, JV., Cioslowski, J., Fox, DJ. Gaussian 09 revision C.01. Gaussian Inc; Wallingford, CT: 2010.

15. (a) Becke AD. J. Chem. Phys. 1993; 98:5648.(b) Lee C, Yang W, Parr RG. Phys. Rev. B. 1988; 37:785.

16. (a) Hay PJ, Wadt WR. J. Chem. Phys. 1985; 82:270.(b) Wadt WR, Hay PJ. J. Chem. Phys. 1985; 82:284.(c) Hay PJ, Wadt WR. J. Chem. Phys. 1985; 82:299.

17. (a) Zhao Y, Truhlar DG. Theor. Chem. Acc. 2008; 120:215.(b) Zhao Y, Truhlar DG. Acc. Chem. Res. 2008; 41:157. [PubMed: 18186612]

18. (a) Szentpaly LV, Fuentealba P, Preuss H, Stoll H. Chem. Phys. Lett. 1982; 93:555.(b) Dolg M, Wedig U, Stoll H, Preuss H. J. Chem. Phys. 1987; 86:866.(c) Schwerdtfeger P, Dolg M, Schwarz WHE, Bowmaker GA, Boyd PDW. J. Chem. Phys. 1989; 91:1762.

19. Cossi M, Rega N, Scalmani G, Barone V. J. Comp. Chem. 2003; 24:669. [PubMed: 12666158]

20. CYLview, 1.0b. Legault, C. Y. Université de Sherbrooke; 2009. (http://www.cylview.org)

21. Weigend F, Ahlrichs R. Phys. Chem. Chem. Phys. 2005; 7:3297. [PubMed: 16240044]

22. (a) Lu T, Chen F. J. Comp. Chem. 2012; 33:580. [PubMed: 22162017] (b) Lu T, Chen F. J. Mol. Graph. Model. 2012; 38:314. [PubMed: 23085170]

23. Humphrey W, Dalke A, Schulten K. J. Molec. Graphics. 1996; 14:33. Official website: http://www.ks.uiuc.edu/Research/vmd/.

24. (a) Ye J, Bhatt RK, Falck JR. J. Am. Chem. Soc. 1994; 116:1.(b) Hölzer B, Hoffmann RW. Chem. Commun. 2003:732.(c) Moncarz JR, Brunker TJ, Jewett JC, Orchowski M, Glueck DS, Sommer RD, Lam K-C, Incarvito CD, Concolino TE, Ceccarelli C, Zakharov LN, Rheingold AL. Organometallics. 2003; 22:3205.(d) Campos KR, Klapars A, Waldman JH, Dormer PG, Chen C-Y. J. Am. Chem. Soc. 2006; 128:3538. [PubMed: 16536525] (e) Lange H, Fröhlich R, Hoppe D. Tetrahedron. 2008; 64:9123.(f) Saito B, Fu GC. J. Am. Chem. Soc. 2008; 130:6694. [PubMed: 18447357] (g) Imao D, Glasspoole BW, Laberge SV, Crudden CM. J. Am. Chem. Soc. 2009; 131:5024. [PubMed: 19301820] (h) Li H, He A, Falck JR, Liebeskind LS. Org. Lett. 2011; 13:3682. [PubMed: 21675755] (i) Taylor BLH, Jarvo ER. J. Org. Chem. 2011; 76:7573. [PubMed: 21797268] (i) Wilsily A, Tramutola F, Owston NA, Fu GC. J. Am. Chem. Soc. 2012; 134:5794. [PubMed: 22443409]

25. For a recent experimental study on the metal-mediated transmetallation with arylborate, see: Thomas AA, Denmark SE. Science. 2016; 352:329. [PubMed: 27081068]

26. The hydrogen atom is appended with a O–H distance of 0.97 Å.

27. The hydrogen atom is appended with a C–H distance of 1.09 Å.

28. (a) Hu X, Castro-Rodriguez I, Olsen K, Meyer K. Organometallics. 2004; 23:755.(b) Zhang X-F, Sun M-J, Cao Z-X. Theor. Chem. Acc. 2016; 135:163.
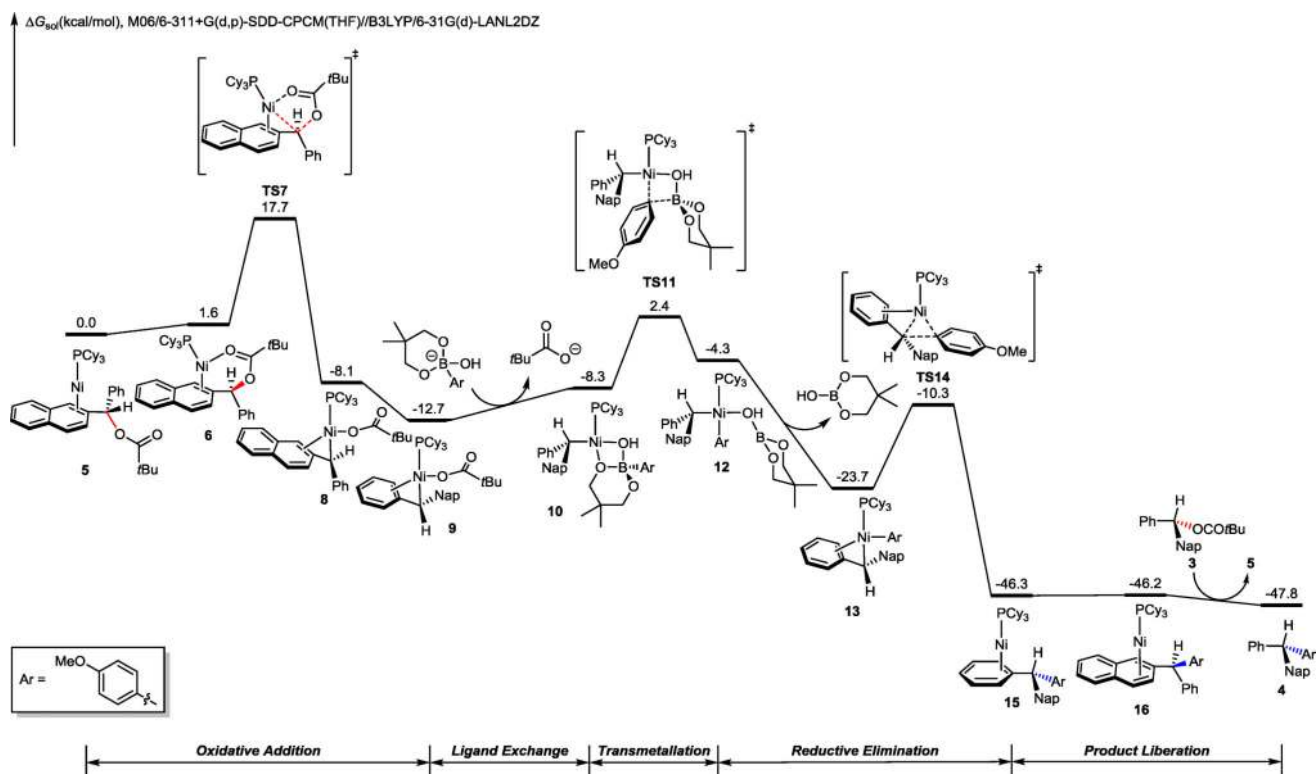
Figure 1.
DFT-computed Gibbs free energy changes of the [Ni(PCy₃)]-catalyzed Suzuki-Miyaura coupling with benzylic ester **3** leading to stereoretention product.
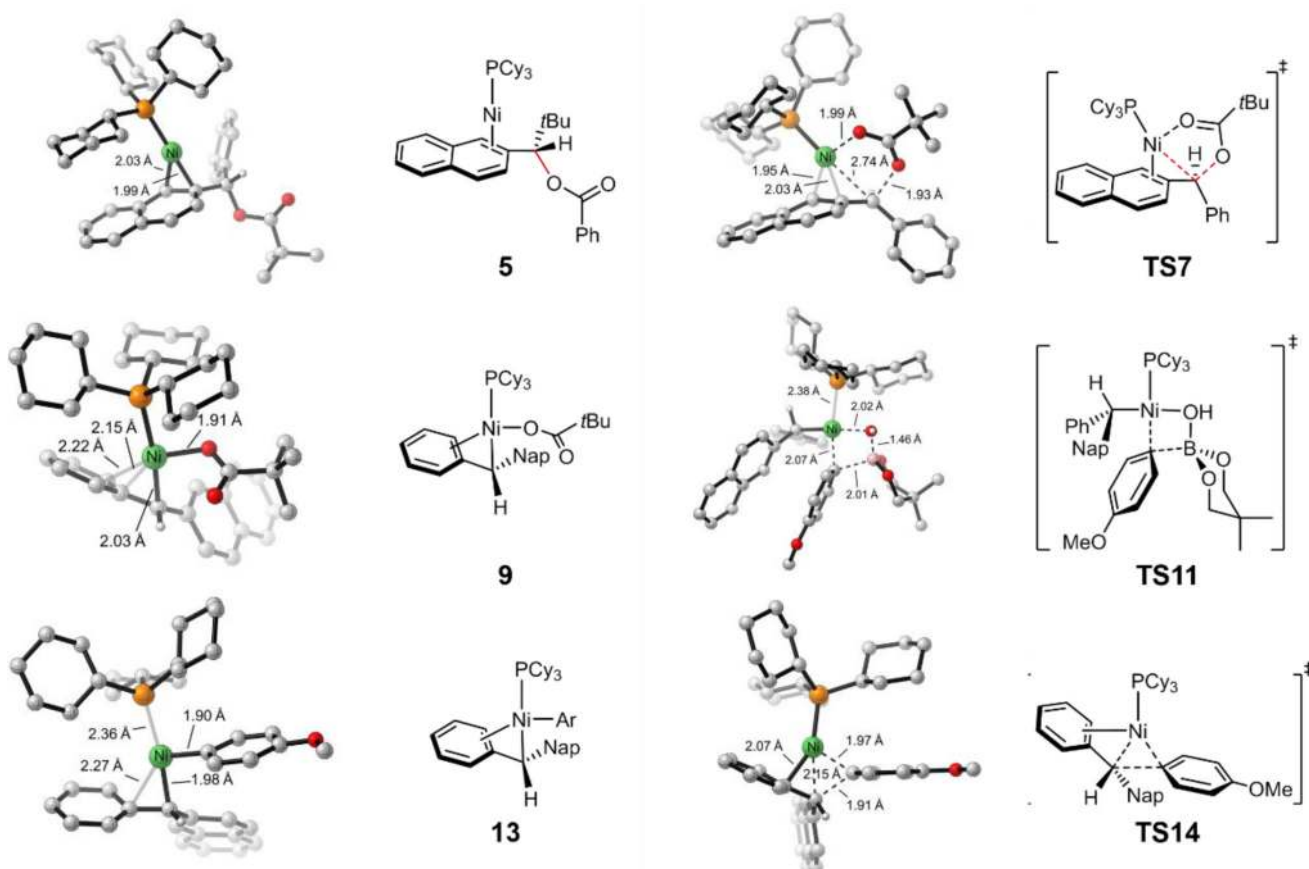
Figure 2.
DFT-optimized structures of selected intermediates and transition states for the [Ni(PCy$_3$)]-catalyzed Suzuki-Miyaura coupling with benzylic ester **3** leading to stereoretention product. All the C–H bonds are hidden for simplicity, except the benzylic stereogenic center.
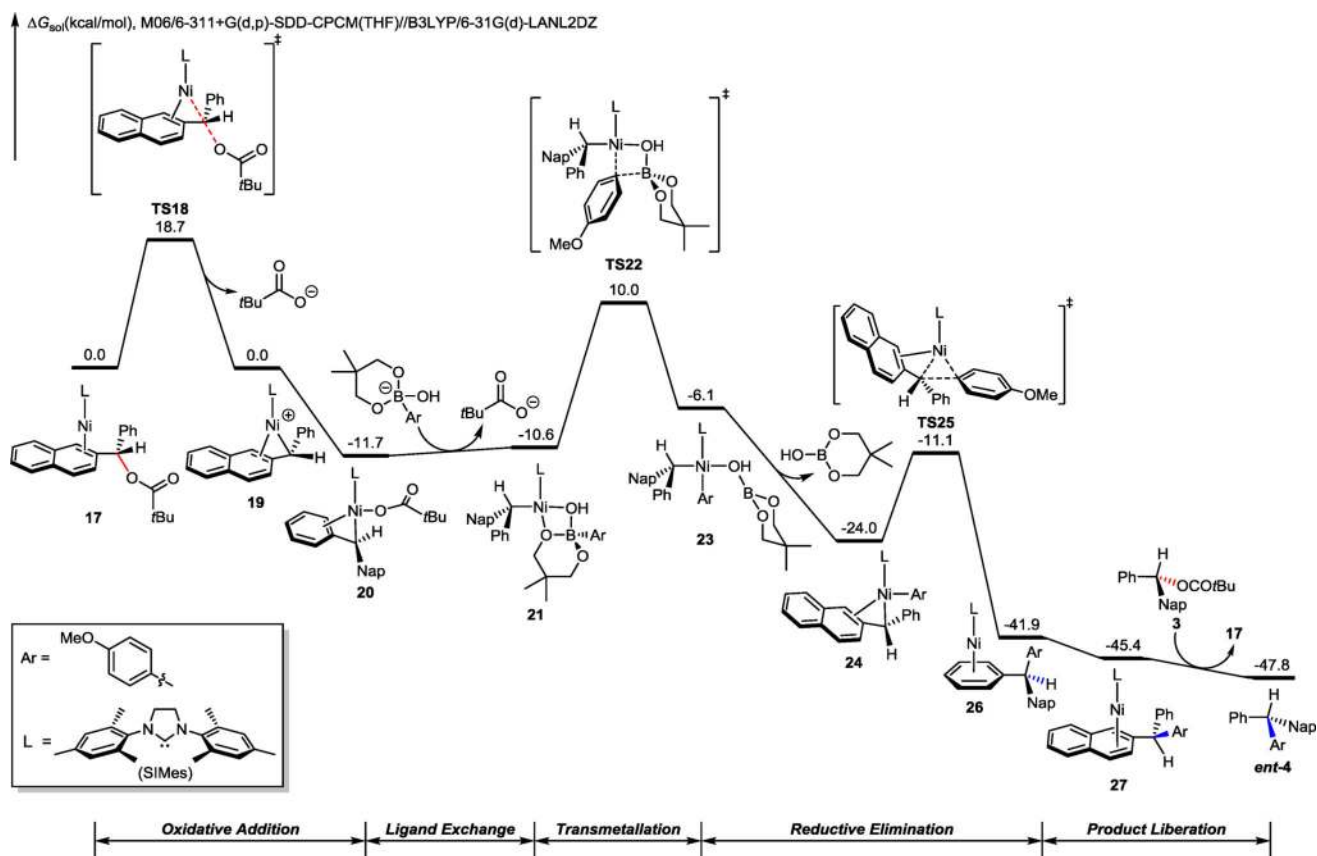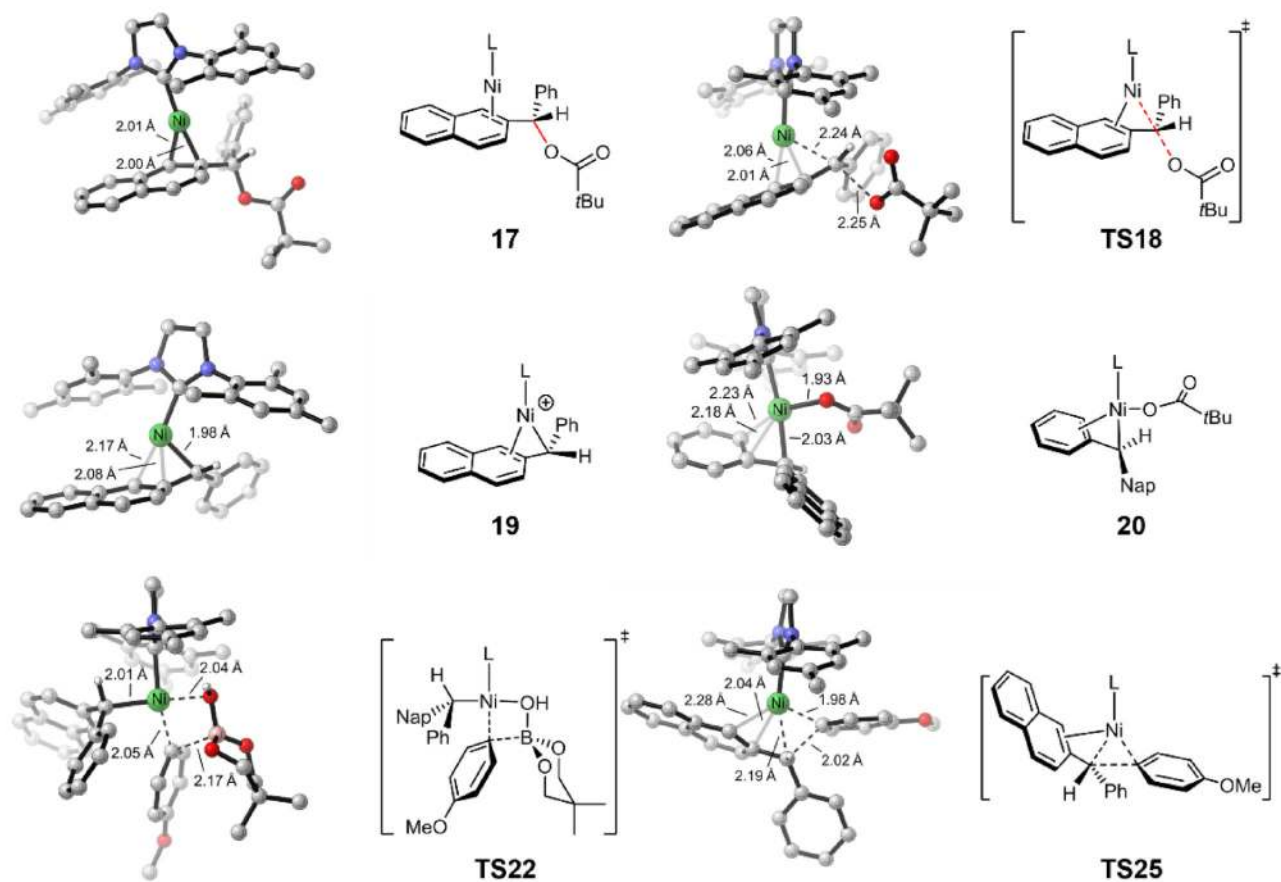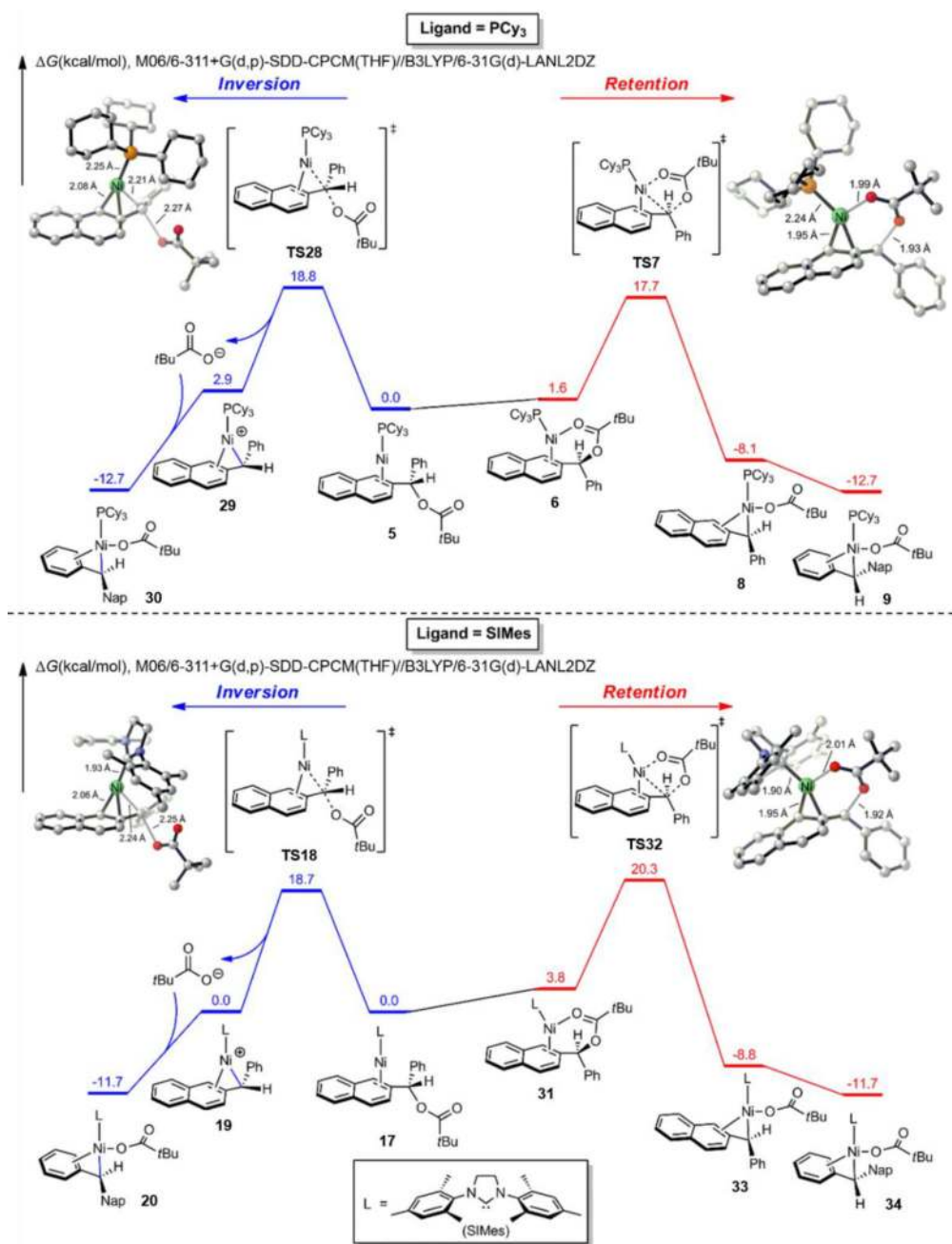
Figure 3.
DFT-computed Gibbs free energies changes of the [Ni(SIMes)]-catalyzed Suzuki-Miyaura cross-coupling with benzylic ester **3** leading to stereoinversion product.

Figure 4.
DFT-optimized structures of selected intermediates and transition states for the [Ni(SIMes)]-catalyzed Suzuki-Miyaura coupling with benzylic ester **3** leading to stereoinversion product. All the C–H bonds are hidden for simplicity, except the benzylic stereogenic center.

Figure 5.
DFT-computed Gibbs free energies changes of the invertive and retentive Ni-mediated oxidative addition of benzylic ester **3** with PCy$_3$ and SIMes ligands.
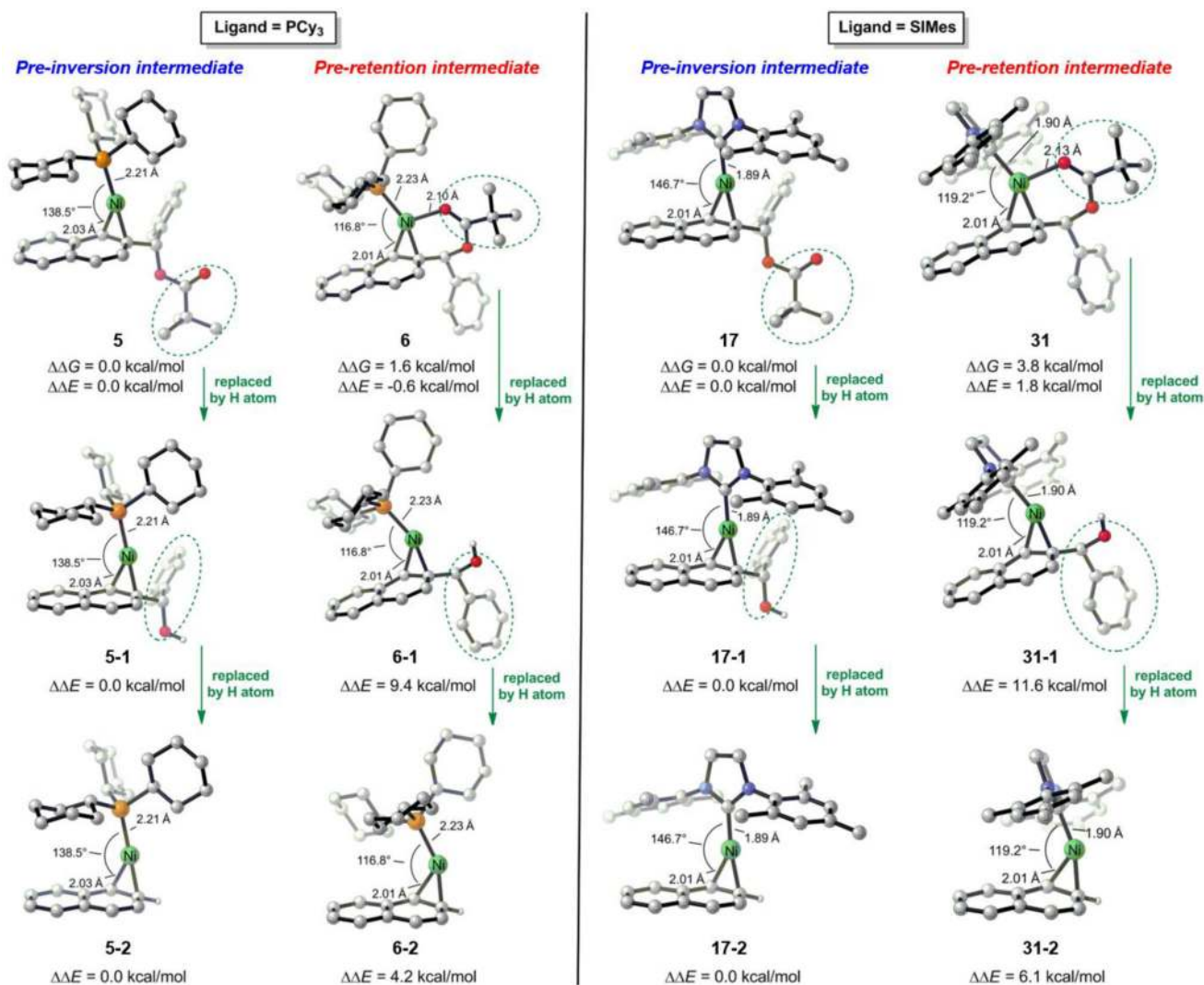
Figure 6.
Energy changes upon replacing groups in the pre-inversion intermediates and pre-retention intermediates with smaller groups to test their roles in determining the stereoselectivities. All H atoms are hidden for simplicity except the ones that are used to degrade the substrates.
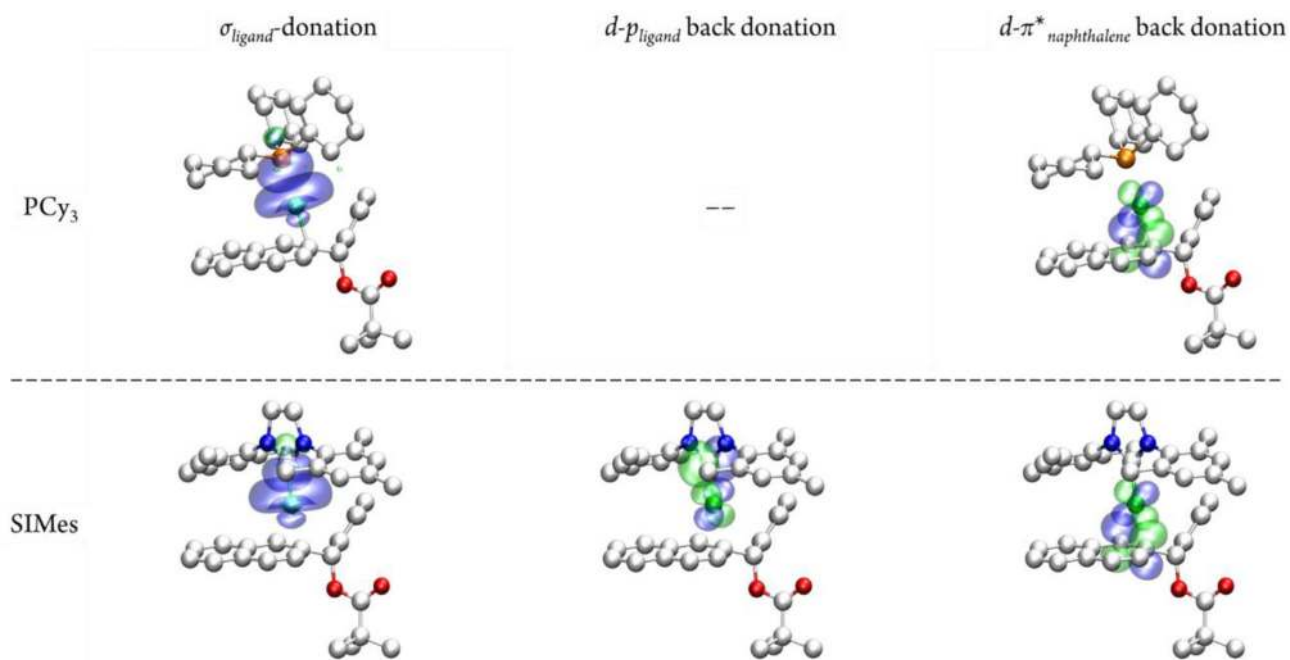
Figure 7.
Major interactions between ligand or pivalate and Ni in [LNi(pivalate)] complexes, calculated with NBO calculation at M06/def2-SVP//B3LYP/LANL2DZ-6-31G(d). The isovalue is 0.05 and all H atoms are hidden for simplicity. The green and blue surfaces represent two opposite phases of the NBOs.
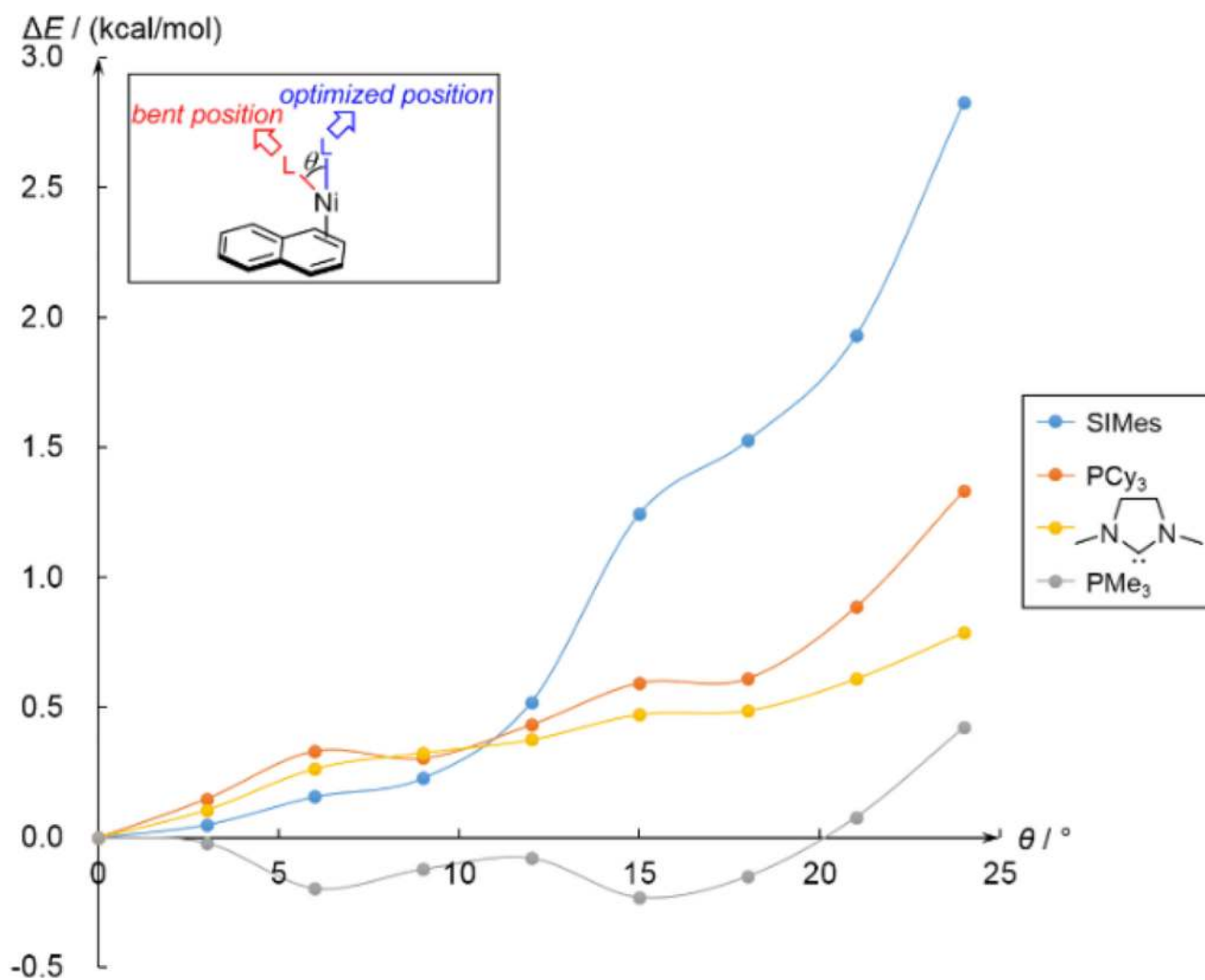
Figure 8.
Relative gas phase electronic energies of [LNi(naphthalene)] complexes with different substrate-nickel-ligand angles. θ is the bending angle of ligand from the optimized position to the bent position.
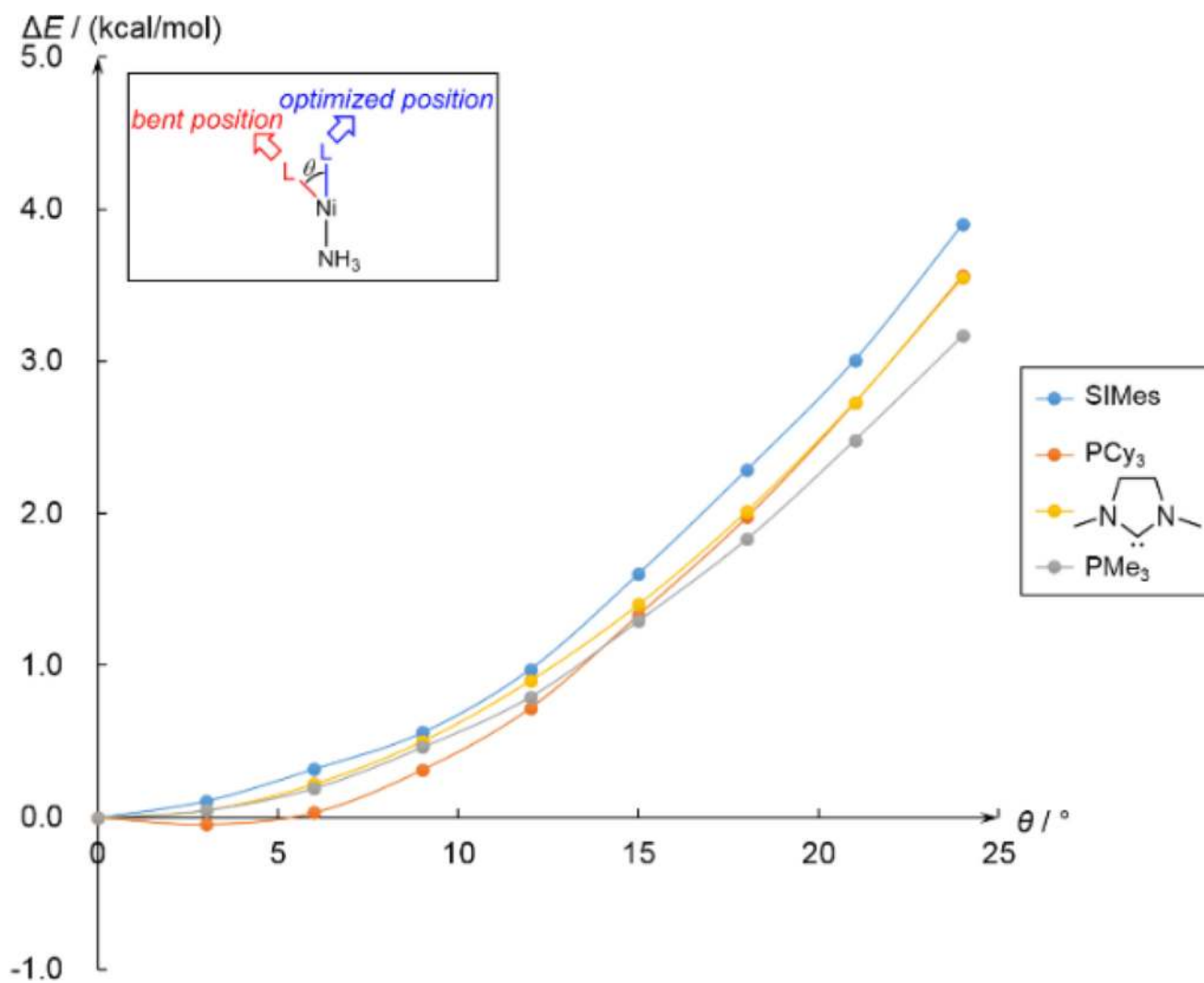
Figure 9.
Relative gas phase electronic energies of [LNi(NH$_3$)] complexes with different substrate-nickel-ligand angles. θ is the bending angle, defined in Figure 8.
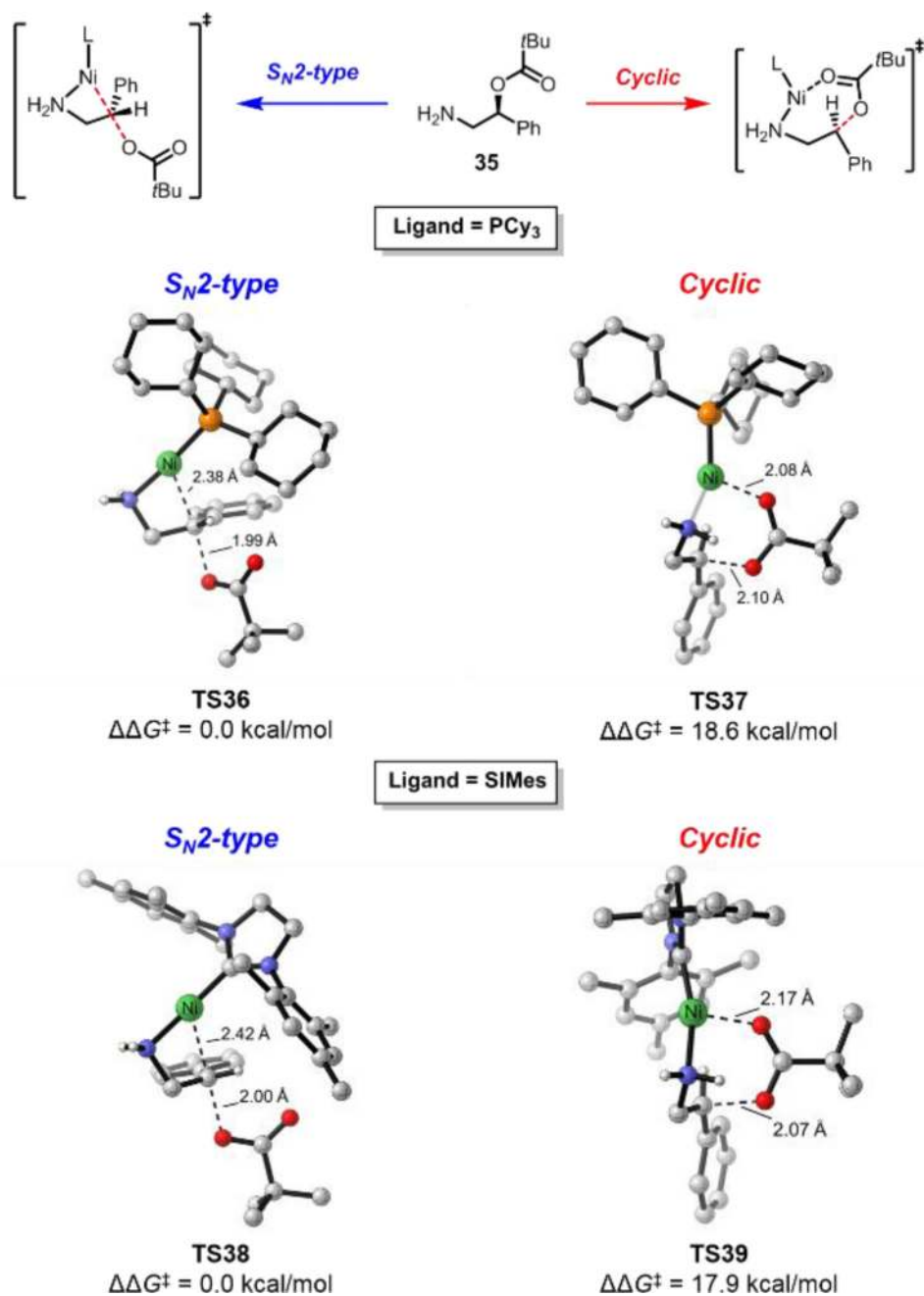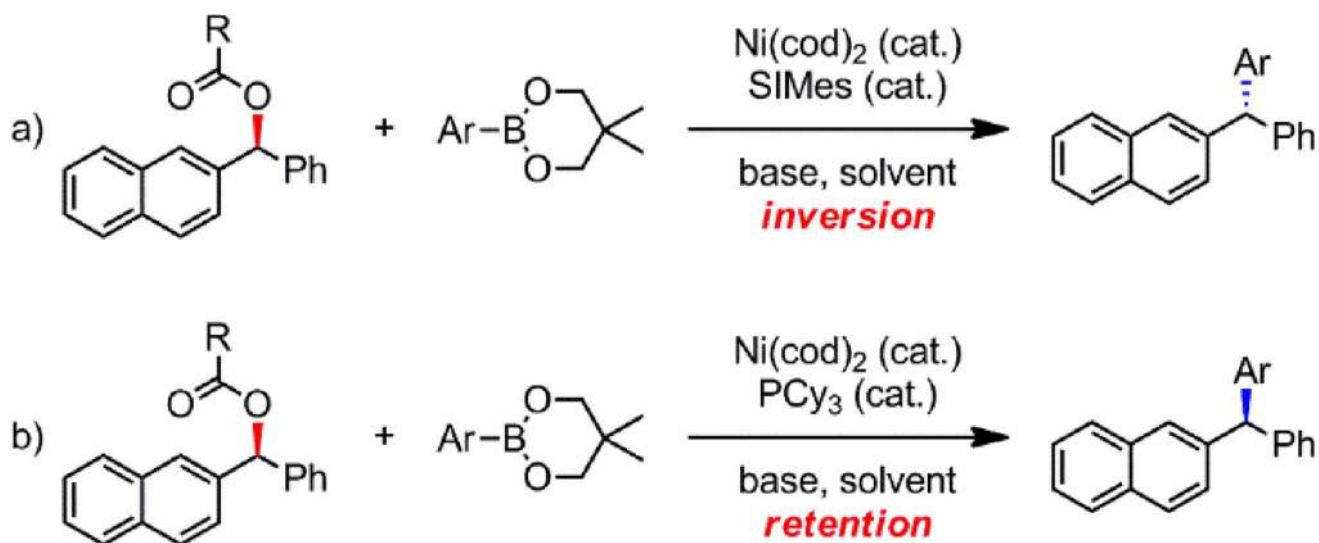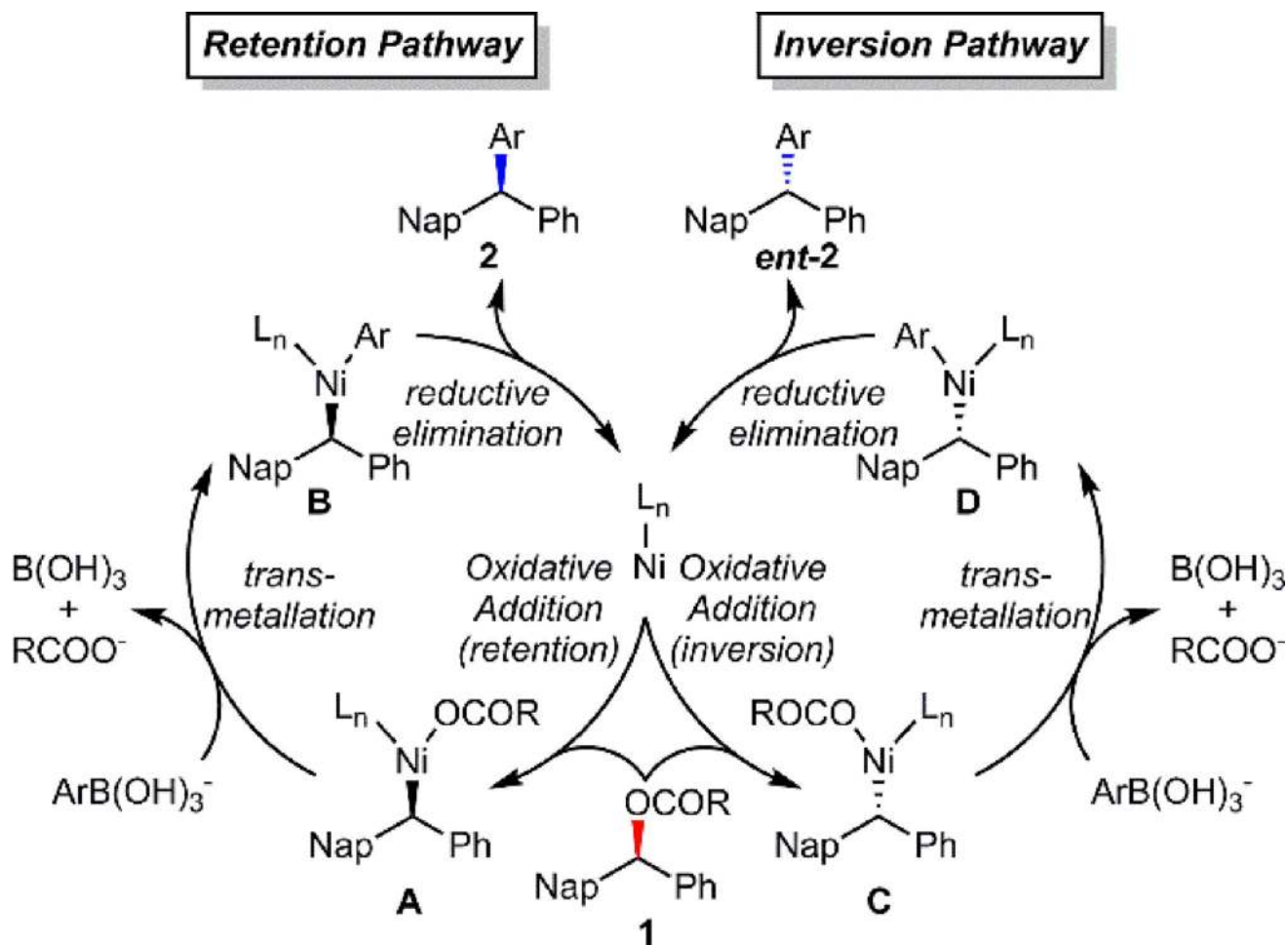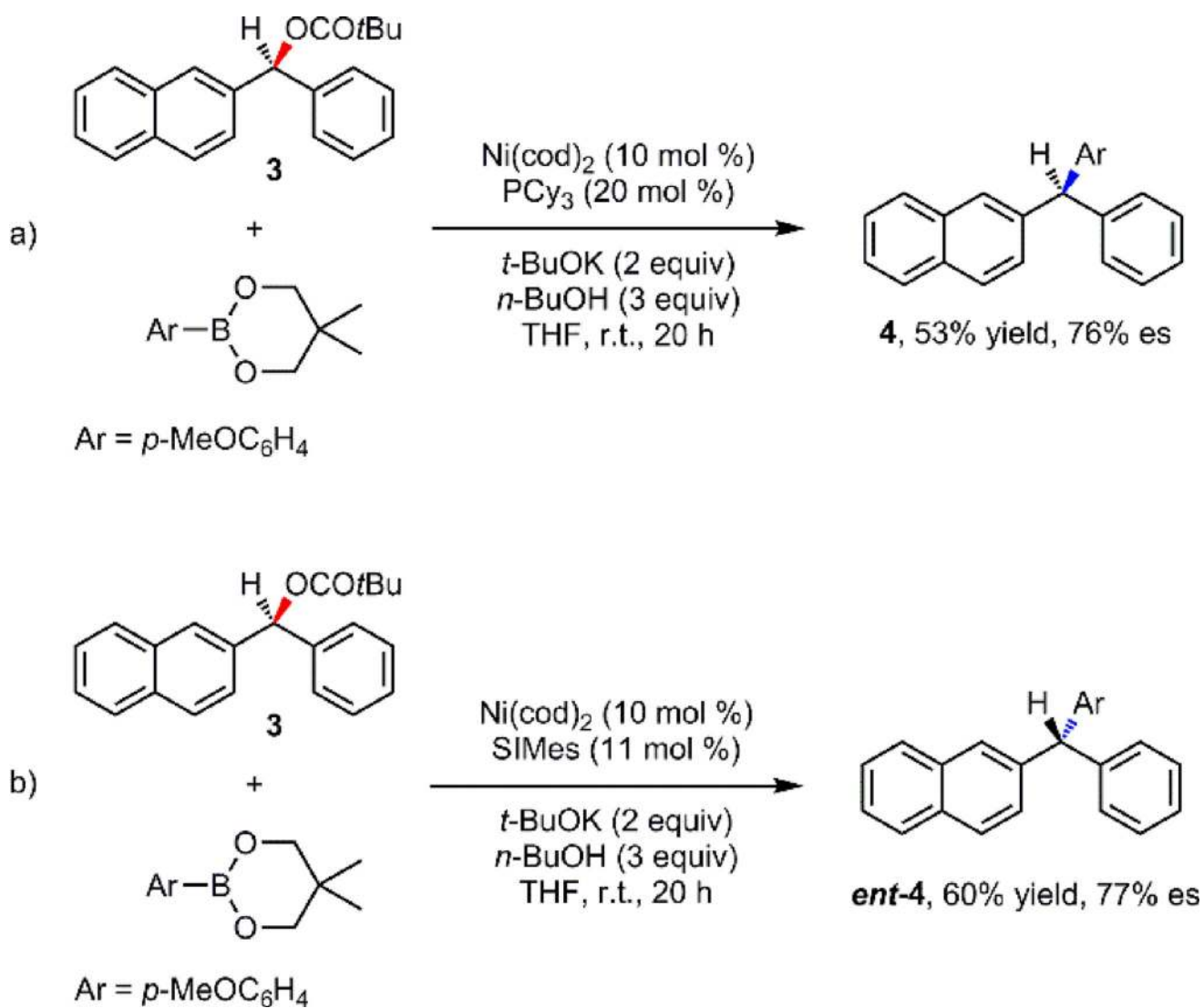
Figure 10.
Optimized structures and relative free energies of the S_N2-type and cyclic C–O cleavage transition states with **35**.

Scheme 1.
Ligand-controlled stereoselectivity in Ni-catalyzed Suzuki-Miyaura coupling reactions with benzylic esters and derivatives.[11d]

Scheme 2.
Proposed mechanisms of stereospecific Ni-catalyzed Suzuki–Miyaura coupling reactions with benzylic ester and derivatives.

a)

H OCOtBu

3

+

Ar—B

Ar = p-MeOC₆H₄

Ni(cod)₂ (10 mol %)
PCy₃ (20 mol %)

————————————→

t-BuOK (2 equiv)
n-BuOH (3 equiv)
THF, r.t., 20 h

H Ar

4, 53% yield, 76% es

b)

H OCOtBu

3

+

Ar—B

Ar = p-MeOC₆H₄

Ni(cod)₂ (10 mol %)
SIMes (11 mol %)

————————————→

t-BuOK (2 equiv)
n-BuOH (3 equiv)
THF, r.t., 20 h

H Ar

ent-4, 60% yield, 77% es

Scheme 3.
Model reactions used for computation.[11d].

$$\Delta\Delta G^{\neq}(\text{PCy}_3) = \Delta G^{\neq}(\textbf{TS28}) - \Delta G^{\neq}(\textbf{TS7}) \qquad \text{eqn 1}$$

$$\Delta G^{\neq}(\textbf{TS28}) = \Delta G(\textbf{5}) + \Delta G^{\neq}(\textbf{5}\rightarrow\textbf{TS28}) \qquad \text{eqn 2}$$

$$\Delta G^{\neq}(\textbf{TS7}) = \Delta G(\textbf{6}) + \Delta G^{\neq}(\textbf{6}\rightarrow\textbf{TS7}) \qquad \text{eqn 3}$$

$$\Delta\Delta G^{\neq}(\text{PCy}_3) = \Delta G^{\neq}(\textbf{5}\rightarrow\textbf{TS28}) - \Delta G(\textbf{6}\rightarrow\textbf{TS7}) - \Delta G_{\text{iso}}(\textbf{5}\rightarrow\textbf{6}) \qquad \text{eqn 4}$$

Scheme 4.
Analysis of the contributions of the stereoselectivity with PCy$_3$ ligand based on Curtin-Hammett principle.

Table 1

Decomposition of the stereoselectivity ($\Delta\Delta G^{\ddagger}$) to the contributions of intrinsic oxidative addition barriers ($\Delta G^{\ddagger}_{\text{intrinsic}}$) and isomerization energy (ΔG_{iso}). Free energies are in kcal/mol.

Ligands	$\Delta G^{\ddagger}_{\text{intrinsic}}$ (inversion)	$\Delta G^{\ddagger}_{\text{intrinsic}}$ (retention)	ΔG_{iso}	$\Delta\Delta G^{\ddagger}$
PCy$_3$	18.8	16.1	1.6	1.1
SIMes	18.7	16.5	3.8	−1.6

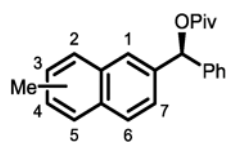## Table 2

Steric effects of substrate and ligand on the stereoselectivity, the computed stereoselectivities are listed as $\Delta\Delta G^{\ddagger} = \Delta G^{\ddagger}(\text{inversion}) - \Delta G^{\ddagger}(\text{retention})$ in kcal/mol.

A. Steric effects of methyl substitution on substrate 3

Substrate	Substitu-ents	$\Delta\Delta G^{\ddagger}$ (PCy$_3$)	$\Delta\Delta G^{\ddagger}$ (SIMes)
	1–Me	3.6	2.4
	2–Me	0.3	−1.7
	3–Me	1.5	−2.7
	4–Me	0.2	−3.4
	5–Me	1.4	−1.9
	6–Me	1.1	−2.8
	7–Me	1.9	−2.7

B. Steric effects of ligand

Substrate	$\Delta\Delta G^{\ddagger}$ (PCy$_3$)	$\Delta\Delta G^{\ddagger}$ (PtBu$_3$)	$\Delta\Delta G^{\ddagger}$ (SIMes)	$\Delta\Delta G^{\ddagger}$ (SIPr)
3	1.1	−3.8	−1.6	−6.2